PAPER • OPEN ACCESS

An overview of negative hydrogen ion sources for accelerators

To cite this article: Dan Faircloth and Scott Lawrie 2018 *New J. Phys.* **20** 025007

New Journal of Physics
The open access journal at the forefront of physics

Deutsche Physikalische Gesellschaft DPG
IOP Institute of Physics

Published in partnership with: Deutsche Physikalische Gesellschaft and the Institute of Physics

OPEN ACCESS

RECEIVED
9 June 2017

REVISED
12 October 2017

ACCEPTED FOR PUBLICATION
21 December 2017

PUBLISHED
15 February 2018

PAPER

An overview of negative hydrogen ion sources for accelerators

Dan Faircloth[1] **and Scott Lawrie**

STFC Rutherford Appleton Laboratory, United Kingdom

[1] Author to whom any correspondence should be addressed.

E-mail: dan.faircloth@stfc.ac.uk

Keywords: negative ion sources, particle accelerators, overview

Abstract

An overview of high current (>1 mA) negative hydrogen ion (H^-) sources that are currently used on particle accelerators. The current understanding of how H^- ions are produced is summarised. Issues relating to caesium usage are explored. The different ways of expressing emittance and beam currents are clarified. Source technology naming conventions are defined and generalised descriptions of each source technology are provided. Examples of currently operating sources are outlined, with their current status and future outlook given. A comparative table is provided.

1. Introduction

Over the last five decades, the negative hydrogen (H^-) ion has become the particle of choice to inject into high power proton accelerator facilities. This is because the ion's charge polarity can be inverted by removing two electrons when it passes through a thin stripping foil, leaving a bare proton. This conversion from H^- ion to proton is known as *charge exchange*. Charge exchange is employed in tandem accelerators to double the accelerating voltage; in cyclotrons to allow simple and effective beam extraction; and in storage rings and rapid-cycling synchrotrons to accumulate high current proton beams. Although using H^- ions brings many advantages to a proton accelerator facility as a whole, the ion source technology required to produce an effective H^- ion beam is more complicated than to produce a proton beam.

A variety of operational H^- ion source technologies are discussed in this paper. Ion sources for accelerator facilities must produce high current beams with low emittance, be highly reliable and have lifetimes compatible with the operating schedule of the accelerator they serve. Depending on the application, the ion beam may either be 'always on' continuous wave (CW) or be pulsed with a range of different pulse lengths, l (in seconds) and repetition rates, f (in Hz). For a pulsed beam, the *duty cycle*, $D = l \cdot f$ describes the proportion of time the ion beam is being produced. Generally, sources operated at lower duty cycles will produce higher pulsed beam currents. For example, pulsed H^- sources typically produce beam currents around 10–80 mA, whereas CW sources typically produce beam currents of 0.5–25 mA. The present drive in H^- research and development is focused on increasing the duty cycle whilst maintaining high beam currents. In addition, caesium has a major role to play in H^- ion production, as will be discussed later, but it brings with it several problems. Therefore another major R&D activity is to reduce the reliance on—or even remove the need for—caesium in H^- ion sources [1–3].

There have been several excellent review papers on the subject of H^- ion sources for accelerators over the years [4, 5]. This paper provides an updated overview of high current (>1 mA) H^- ion sources that are currently providing beam for accelerator facilities or accelerator test stands.

2. H^- ion source fundamentals

2.1. Production mechanisms

It is important to underline that hydrogen has an electron affinity of only 0.7542 eV. Considering that the electron binding energy of neutral hydrogen is 13.6 eV, the extra electron on an H^- ion is very loosely held on.

The negative hydrogen ion production mechanisms, as they are currently understood, can be separated into two main branches: *surface* and *volume* production. Surface production requires a positive ion or an energetic (or a hyper-thermal) neutral hydrogen atom to impact a low work function material. At the surface, the impacting particle may capture electrons and form a negative ion. The rate of electron capture becomes high enough at short distances that the incoming particle loses memory of its original charge, so it suffices to assume that surface-produced negative ions are always formed from neutral atoms. Similar to the ionisation energy required to remove an electron from a neutral atom, there exists an *affinity* energy, which is the energy released when an extra electron is added to an already neutral atom. Generally, the electron affinity is much lower than the ionisation energy, so negative ions are very fragile and easy to *strip*. In the moments before impact, the wave functions of the surface and impacting atom overlap, resulting in the electron affinity level of the atom smoothly shifting downwards toward the valence band of the surface. Valence electrons may then tunnel onto the atom with an exponentially higher likelihood as the atom moves closer to the surface [6, 7]. If the surface material has a low *work function*, the affinity does not need to shift down so far before electron capture occurs. The low work function affects H^- formation probability not only due to the required affinity shift but also due to increased tunnelling probability of the electron through the surface potential barrier. The material with the lowest work function is caesium. Therefore, H^- ion sources dominated by surface production generally involve the introduction of caesium to reduce the surface work function as much as possible [8].

Volume production of H^- ions is a two-step process:

$$H_2 + e(\text{fast}) \rightarrow H_2{}^* + e(\text{slow}),$$

$$H_2{}^* + e(\text{slow}) \rightarrow H^- + H^0.$$

The first step is to create population of highly excited ro-vibrational hydrogen molecules. These are made both by colliding ground-state H_2 with fast electrons and also at the walls of the plasma chamber. The second step is dissociative attachment of slow (~1 eV) electrons with the $H_2{}^*$. The cross section of the dissociative electron attachment process depends strongly on the vibrational level of the H_2 molecule and the energy of the impacting electron. This is because the probability of the compound state to dissociate into H and H^- without auto ionisation depends strongly on the inter-nuclear distance which is affected by the vibrational energy.

To successfully form H^- ions using the volume technique, a magnetic *filter field* is required inside the ion source which divides the plasma into two distinct regions: a high-temperature region to create excited molecules and a low-temperature region near the outlet aperture to create and quickly extract the H^- ions [9]. A filter field of around 10 mT is sufficient to reflect high energy electrons but allow slow electrons and hydrogen to diffuse across toward the extraction region.

Until recently, H^- ion sources were categorised as purely surface or volume sources. For example, Penning [10], magnetron [11] and surface-converter [12] sources primarily create H^- ions from caesiated cathodes; whereas filament [13] and RF [14] sources use the volume technique. However for high power applications, new ion sources increasingly combine both techniques [15–17]. They achieve this in a low-pressure plasma with an optimised filter field for favourable volume production, but enhance the H^- yield with a caesiated extraction aperture. Excellent source cleanliness and a well-understood caesium conditioning process are vital for operation of these hybrid sources.

There are many processes that can destroy H^- ions. The most common are:

$$H^- + H^+ \rightarrow H^0 + H^0 \quad \text{mutual neutralization},$$

$$H^- + e \rightarrow H^0 + 2e \quad \text{electron detachment},$$

$$H^- + H^0 \rightarrow H_2{}^* + e \quad \text{associative detachment}.$$

The cross section of the H^- ion in these destruction processes is also larger compared to the H^0 atom. As well as being fragile and easily destroyed, it is more likely to be hit. The aim of the H^- ion source designer is to minimise the H^- destruction processes by controlling the geometry, temperature, pressure and fields in the source.

2.2. On caesium handling

The use of caesium (Cs) is itself an interesting topic. Due to its low work function, Cs is often added to H^- ion sources to enhance the rate of surface production. As Cs atoms are deposited on (typically) a molybdenum (Mo) surface, the work function decreases from 4.6 eV for Mo toward 2.1 eV for bulk Cs. When the surface is partially covered, however, the work function actually has a minimum of 1.5 eV: lower than that of Cs or Mo. This minimum occurs at a Cs coverage factor somewhere between 0.5 and 0.7 monolayers [18]. Maintaining the optimal surface coverage is of paramount importance to an H^- ion source operator [19]. Several techniques are in use.

At its most simple, elemental Cs with a purity of at least 99.99% may be housed in a heated *oven* (often the misnomer 'boiler' is used for this device: although the Cs is fully melted in the oven, it is far from its boiling point). Caesium is in the liquid state at 28.4 °C. Operating the oven at around 150 °C yields a significant flux of Cs vapour from the oven into the ion source via a heated *transport* tube. The transport tube is maintained at around 300 °C so that it is the hottest point in the transport system, preventing Cs accumulating [20], possibly leading to a blockage. Caesium is highly reactive to oxygen and water vapour in the atmosphere, so care must be taken especially if elemental Cs is used. The Cs may be installed into the oven sealed inside a glass ampoule, which is cracked under an inert gas at atmospheric pressure after the ion source is installed on the accelerator. This prevents any risk of personnel handling exposed Cs. Alternatively the ampoule may be heated (to melting point) and cracked inside a secure and inert gas glove box [21], then carefully poured into the oven before being attached to the ion source. Although more difficult and with higher associated risks, this method ensures that no partially-cracked glass blocks the flux of Cs into the ion source [22]. In either method, the oven must be well cleaned and baked out to remove any impurities which could affect the Cs. The oven and transport tube should be well insulated to contain the required heat. This can be done either by wrapping insulating tape around the assembly, or by constructing a bespoke insulating jacket. The oven and transport tube may be separated with an all-metal shut-off valve which can survive the high temperatures. With the valve closed, the oven can be removed, thus allowing separate filling or maintenance of either the oven or the source. However the valve does add complexity to the caesium transport system and may not be suitable for every application.

Alternative methods of dispensing Cs are also well practised. Caesium-chromate cartridges may be used instead, which are very stable even at elevated temperatures. The cartridges contain a Zr–Al getter, which reduces the Cs_2CrO_4 to Cs, Al_2O_3, Cr_2O_3, and ZrO_2 when heated to >500 °C without the emission of any gaseous products. The cartridges emit a known flux of Cs when heated, albeit at a much higher temperature than elemental Cs [23]. Caesium-chromate cartridges may be installed directly inside the ion source [24], without the need of a remote heated transport system. In this manner, the Cs is already located near where it needs to be on the cathode surfaces and so much less excess vapour is wasted or emitted into locations where it would have an adverse effect. An alternative method is to pass an electrical current of several Ampères through a solid Bi_2Cs dispenser which releases a Cs on demand [25]. The Cs flux can be measured directly at the dispenser opening using a surface ionisation detector for highly accurate control of the Cs evaporation rate.

Regardless of how Cs is injected into the ion source, it must usually be replenished because the plasma sputters away Cs atoms deposited on the cathode. The replenishment is also required to bury 'impurities' (sputtered metal from the walls, metal eroded from the filaments etc) under a fresh Cs layer on the H^- production surface.

The sought-after minimum work function is actually difficult to achieve in test stands [26], while in real ion sources with plasma this minimum is often reached by varying the temperature of the H^- emitting surface. Since the Cs must usually be continuously injected into the ion source, one might naturally ask where it ends up. For example, typical elemental Cs ovens hold several grams of caesium, which evidently does not remain on the source cathode. In fact usually the Cs escapes the ion source and enters the high voltage extraction region, covering it and the rest of the vacuum vessel. Caesium depositing on negative high voltage electrodes drastically enhances the rate of sparking, so a careful control of Cs flux is required, as well as shielded insulators and heated electrodes to prevent Cs accumulation [27]. One noteworthy exception is the SNS ion source which has a well-rehearsed caesiation procedure to ensure the surface-production collar is extremely clean and free of impurities. This allows Cs atoms to bind sufficiently strongly to the surface to prevent sputtering [28]. In this manner, no additional Cs needs to be injected into the source after the initial caesiation on start-up: a significant achievement.

Variation in caseation can have a significant effect on source performance. It should also be noted that the total Cs consumption throughout the source lifetime varies hugely depending on the type of source technology: Penning and magnetron surface plasma sources can use >10 g, whereas the SNS source only uses a few mg.

2.3. Beam emittance

As well as the headline figures of beam current, duty-cycle and lifetime, the transverse emittance is a very important number to quote for each ion source. An ion source may be able to produce 100 mA of beam current, but if it has such a large emittance that it cannot be transported through the rest of the accelerator, then it is of no practical use. Unfortunately, the emittance often causes confusion and makes comparison between sources difficult as there are many ways to quantify it. H^- ion beams can seldom be defined with simple Gaussian distributions, since the beam current density is often perturbed by magnetic filter fields, electron-dumping fields or other asymmetries in the extraction system. Kapchinskij–Vladimirskij (KV) [29], bi-Gaussian or waterbag distributions may be used to analytically describe the more complicated beams. Often there are halo particles, nonlinear tails or 'ghost beams' overlapping the main beam distribution in *trace space*. Outlying particles have a

disproportionally large influence on the overall measured emittance. Therefore sometimes some *threshold* is chosen to cut out the bottom few percent of the data such that it is not included in the emittance calculation. Then one must be careful to indicate exactly what fraction of the beam is included [30]; for example 90% or 95% emittances are often quoted. Conversion factors can be calculated for different emittance values; for example the 95% emittance is equal to six times the RMS emittance, whereas a KV distribution is equal to four times the RMS.

The four-RMS emittance has become somewhat of a standard in the accelerator community after the proposal by Lapostolle [31], so it is adopted in this paper. For a statistical ensemble $I(x,\ x')$ of particle intensities passing through positions x at angles x', the 4·RMS emittance is defined by the second moments of the distribution:

$$\varepsilon_{4\mathrm{RMS}} = 4 \cdot \sqrt{\langle x^2\rangle \langle x'^2\rangle - \langle xx'\rangle^2}\,,$$

where: $\langle x^2\rangle = \frac{\sum_{\mathrm{all}} x^2 I(x,x')}{\sum_{\mathrm{all}} I(x,x')}$, $\langle x'^2\rangle = \frac{\sum_{\mathrm{all}} x'^2 I(x,x')}{\sum_{\mathrm{all}} I(x,x')}$ and $\langle xx'\rangle = \frac{\sum_{\mathrm{all}} xx' I(x,x')}{\sum_{\mathrm{all}} I(x,x')}$.

Before calculating the second moments, the distribution should be normalised to its centroid to eliminate the first moments. That is, each position x and angle x' in the equations above are equal to $(x_0 - \langle x_0\rangle)$ and $(x'_0 - \langle x'_0\rangle)$, respectively, where x_0 and x'_0 are the raw measured positions and angles, whereas

$$\langle x_0\rangle = \frac{\sum_{\mathrm{all}} x_0 I(x_0,\ x_0')}{\sum_{\mathrm{all}} I(x_0,\ x_0')} \text{ and } x'_0 = \frac{\sum_{\mathrm{all}} x'_0 I(x_0,\ x_0')}{\sum_{\mathrm{all}} I(x_0,\ x_0')}$$

are the first moments, or means. Since all ion sources produce beams of different energies, the 4·RMS emittance values quoted herein are normalised to the particle velocity for easy comparison, thus:

$$\varepsilon^{\mathrm{norm.}}_{4\mathrm{RMS}} = \beta\ \gamma\ \varepsilon_{4\mathrm{RMS}},$$

where β and γ are the usual relativistic velocity factors. The self-consistent un-biased elliptical exclusion analysis [32] is a useful technique to accurately calculate the 4·RMS emittance even in the presence of low-level background or ghost particles discussed above, without having to take arbitrary thresholds.

4-RMS emittance is a meaningful value to quote because it contains around 90% of the beam (89%–100%), regardless of the distribution (Gaussian, KV, waterbag, s-shapes etc), whereas 1-RMS contains 25%–40% of the beam, depending on the distribution. This is a much more significant variance which can give a misleading impression of the beam's quality. For clarity, the 4-RMS emittance is a value, which when multiplied by π, is an area in the phase space which contains 90% of the beam. By explicitly including π in the units, there is no confusion that it is an emittance area. Similarly, some people fold the milliradian (a simple ratio equalling 0.001) into the mm unit, compressing mm mrad down to μm which can also cause confusion.

2.4. Beam current

As well as being careful to indicate the correct emittance, the beam current can also cause confusion. For example, the ion source may produce a beam current which is not fully transported through the subsequent low energy beam transport (LEBT) and later accelerating stages. Therefore one might ask whether to only report the transportable beam current, or the current which fits inside the accelerator acceptance. This measurement is usually difficult to determine online in an operational facility, rather than on a test stand with multiple diagnostics devices. Moreover, transportation problems are usually attributed to unknown LEBT space-charge compensation or a poorly performing radio frequency quadrupole (RFQ), not to the ion source itself. Therefore, to ensure consistency, all values reported in this paper refer to the H^- beam current delivered to the entrance of the LEBT by the ion source.

The actual measurement of beam currents from negative ion sources is also fraught with problems because of electrons. Electrons co-extracted from the source can be inadvertently transported to the measurement. If the pressure is high enough electrons from background gas stripping can be measured. Secondary electrons from beam lost on structures in the vessel can be measured. Beam current toroids can read high or low depending on what direction these stray electron currents are flowing through them. Interceptive Faraday cups need careful design and setup with secondary electron suppression and adequate electrical screening.

3. Source technologies

3.1. Classification

Source technology is classified by how the primary plasma discharge is driven and by the dominant H^- production processes. Surface, volume and charge exchange processes will occur in all sources to differing degrees. The terminologies shown in **bold** are used to classify the different source technologies.

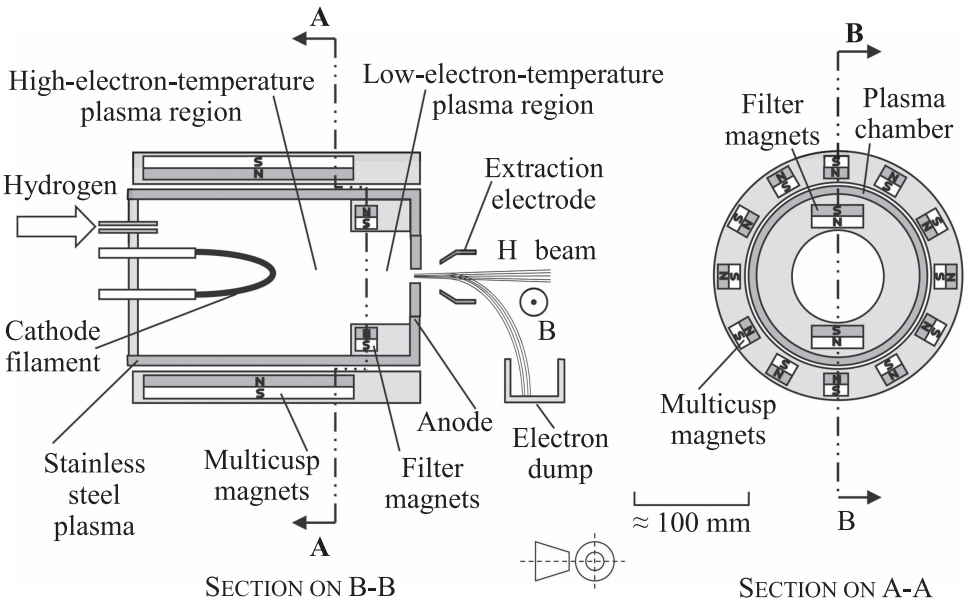

Figure 1. Schematic of a filament driven volume source.

All accelerator facility H^- ion sources generate their primary plasma by electron impact ionisation driven by an electrical power source. The electrical power can be electrostatically coupled to the plasma via the electric field or inductively coupled by the magnetic field. The power source can be a current regulated power supply that applies a voltage between the cathode and anode electrodes, or power regulated amplifier that couples to the plasma via an **antenna** or **waveguide.**

The electrodes can be cooled, or run hot, or be heated to visibly high temperatures as in a cathode **filament**. The electrodes form the walls of the plasma chamber in the **Penning** and **magnetron** geometries. The other sources have a plasma-confining **multicusp**-magnetic-field surrounding the plasma chamber, this allows the walls of the chamber to be constructed of conducting or non-conducting material. The multicusp field also helps to improve the power efficiency by confining the energetic electrons.

The power supply must be capable of applying enough voltage to overcome the strike potential and then to be able to regulate with a non-Ohm's law load. The power supply must also be able to withstand short circuits.

For **RF** (MHz) or **microwave** (GHz) sources, the amplifier driving the plasma is power regulated and it must be able to withstand reflected power. The **antenna** or **waveguide** can be immersed in the plasma, **internal** to the plasma chamber; or it can be outside the plasma, **external** to the plasma chamber. Keeping the antenna out of the plasma reduces sputtering erosion problems and can yield sources with very long lifetimes, however it can require higher output power from the amplifier due to lower coupling efficiency to the plasma. The antenna geometry is most commonly a **solenoidal** helix or a **planar** spiral.

Volume production requires the presence of magnetic filter fields to stop fast electrons. **Surface** production becomes significant when caesium is present in the source. **Surface Plasma** is an accepted term for the surface and resonant charge exchange processes that occur in Penning and magnetron sources. **Surface Converter** sources require a caesiated surface biased at a negative voltage.

The following sections provide generalised descriptions for each of the source technologies and give current examples of their implementation.

3.2. Filament driven volume (and surface) sources

3.2.1. Generalised description

The filament driven volume source has a cylindrical plasma discharge with a magnetic dipole filter field near the emission aperture as shown in figure 1. The dipole filter field creates a region of low electron temperature near the emission aperture allowing H^- volume production.

Hydrogen is fed into the discharge through an opening. The plasma chamber wall is the anode and a heated filament is the cathode. The plasma discharge is created by applying power between the anode and cathode using either a voltage or current regulated power supply:

For the plasma driven with tungsten (W) or tantalum (Ta) filaments, a voltage regulated power supply is used, since the discharge current is regulated by the operation with the space-charge-limited electron-emission mode by using the W or Ta filaments with a sufficiently high temperature. On the other hand, the current

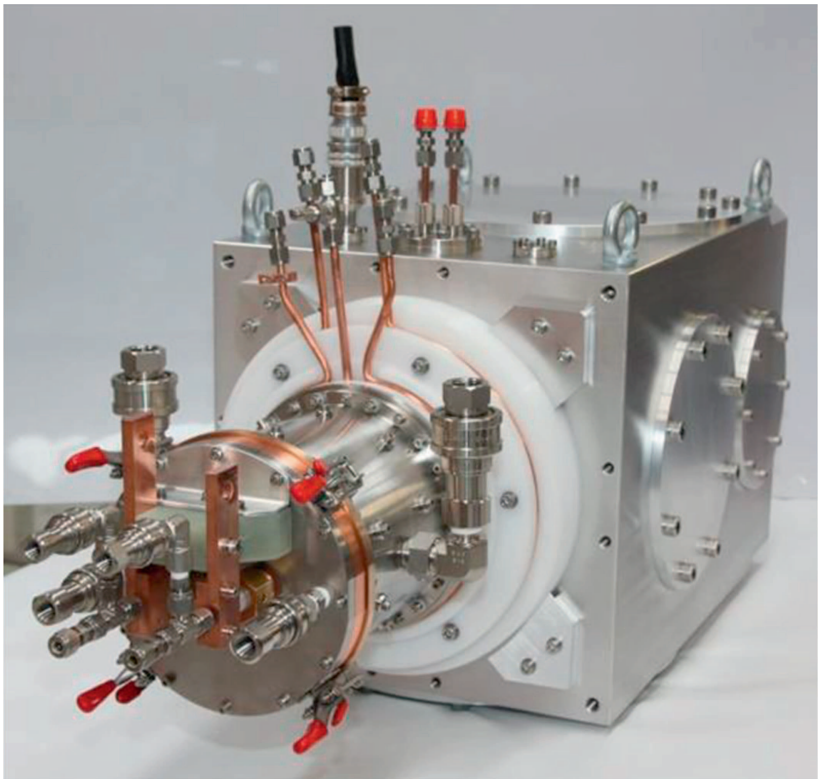

Figure 2. D-Pace filament-driven volume source and vacuum vessel. Reproduced with permission from Dehnel – Particle Accelerator Components & Engineering, Inc.

regulated power supply is essential for the plasma driven with a Lanthanum hexaboride (LaB_6) filament, since the LaB_6 filament is operated at a temperature much lower than that for the space-charge limited electron-emission mode.

The walls of the vessel are lined with a multicusp magnetic field arrangement to confine the plasma.

Caesium can be added to this source to make it a combined Volume and Surface source. The addition of caesium increases the H^- beam current and reduces the co-extracted electron current.

3.2.2. D-Pace filament source, Canada

Based on the source design developed at the TRIUMF cyclotron in Canada [13], this source is commercially available to purchase from D-Pace as a complete 'turnkey' system [33]. Shown in figure 2, it is now in use at many accelerator facilities. When configured with four 1.6 mm diameter tantalum filaments arranged in concentric half circles and 5 kW of discharge power, this source is able to produce up to 18 mA CW H^- beams.

3.2.3. Sumitomo heavy industries, caesiated filament driven multicusp source. Japan

A caesiated filament-driven multicusp H^- source is being developed for medical cyclotrons at Sumitomo Heavy Industries. The source can produce 23 mA CW beams [34].

3.3. External planar RF antenna driven volume sources

3.3.1. Generalised description

The external planar RF antenna driven volume source has a cylindrical plasma discharge with a magnetic dipole filter field near the emission aperture. The plasma discharge is coupled to a flat spiral RF antenna behind a dielectric RF window as shown in figure 3.

Hydrogen is fed into the discharge through a hole. The plasma discharge is created by applying power via the antenna using a power regulated amplifier. The walls of the vessel are lined with a multicusp magnetic field arrangement to confine the plasma.

3.3.2. D-Pace RF source, Canada

This source is based on the filament driven source described in the previous section 3.2.2, in which an external planer RF antenna developed by the University of Jyväskylä, Finland [35]. This source is also commercially available to purchase from D-Pace as a complete 'turnkey' system [36]. With a 3 kW 13.56 MHz RF discharge,

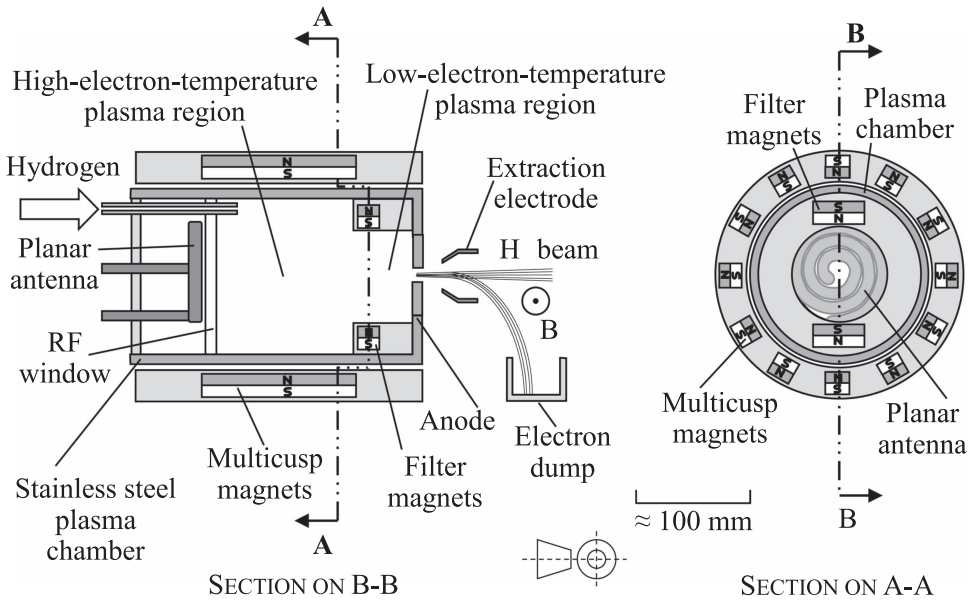

Figure 3. Schematic of an external planar RF antenna driven volume source.

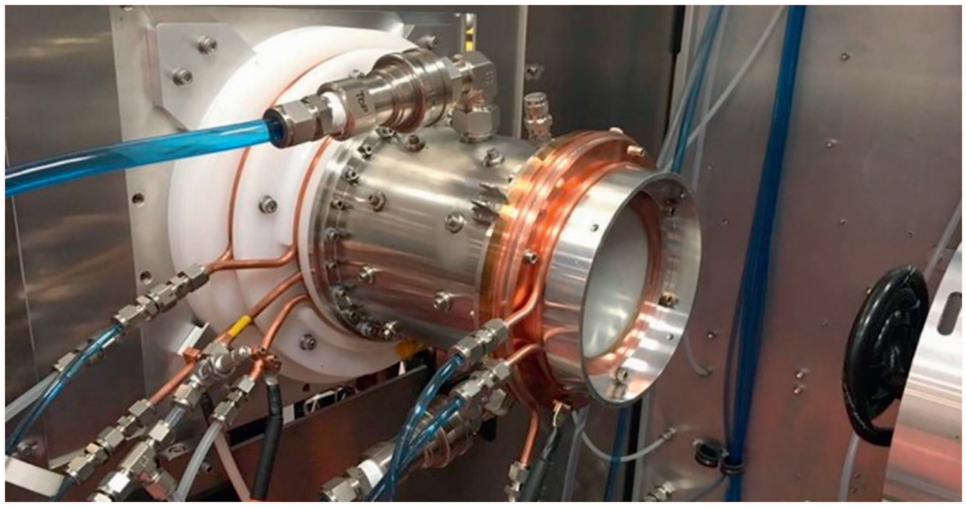

Figure 4. D-Pace RF source with planar RF antenna (black) removed to the right to show RF window. Reproduced with permission from Dehnel – Particle Accelerator Components & Engineering, Inc.

this source can produce up to 8 mA CW H^- beams. A simple aluminium-nitride RF window (shown in figure 4) is the only relatively-fragile plasma-facing part; so long lifetimes in excess of 1 year are expected.

Both the D-Pace RF and filament sources can be run with deuterium or Acetylene for D^- and C_2^- beams, respectively [37].

3.4. Microwave driven volume sources

3.4.1. Generalised description

The microwave driven volume source (figure 5) has a cylindrical plasma discharge with a magnetic dipole filter field near the emission aperture. The microwave power is coupled to the plasma discharge via a waveguide either with a stepped matching section or through a dielectric window.

Hydrogen is fed into the discharge through a hole. The walls of the vessel are lined with a multicusp magnetic field arrangement to confine the plasma.

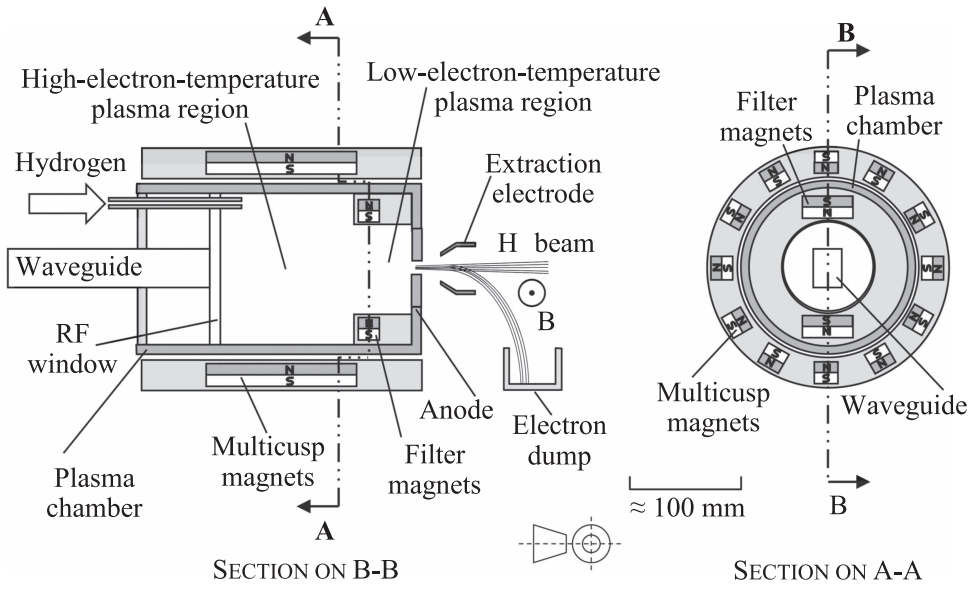

Figure 5. Schematic of microwave driven volume source.

3.4.2. Peking University (PKU) microwave source

PKU is currently developing a microwave driven volume source with a cooled RF window. On an ion source test stand, they have recently reported over 25 mA of CW H^- beam current without the addition of caesium [38]. The previously highest reported CW currents for this type of source are 5 mA at Argonne National Laboratory [39] and 3.8 mA CEA Saclay [40]. If PKU can demonstrate that 25 mA of CW H^- beam current can be transported to an accelerator, this will become the leading long-lifetime source technology.

3.5. Magnetron surface plasma sources

3.5.1. Generalised description

The magnetron surface plasma source shown in figure 6, has a discharge that twines around a central reel-like cathode like a belt. The cathode is held inside the anode body using a ceramic insulator. Caesium vapour from an external oven and hydrogen are fed into the discharge through holes in the anode body. A magnetic field is applied parallel to the axis of the reel-like cathode; this causes the electrons to propagate around the belt-like discharge. Power is applied to the discharge between the anode and cathode. Beam is extracted through a hole in the anode. Often there is an indent (dimple) in the cathode opposite the extraction hole that increases the output current by focusing cathode produced H^- towards the extraction hole. An extraction electrode is used to create the electric field that extracts and shapes the beam from the extraction aperture. A large proportion of the H^- beam is directly extracted from the focusing dimple at cathode potential without undergoing resonant charge exchange with slow H^0, this means magnetrons have somewhat higher beam noise and energy spread than Penning ion sources discussed later.

3.5.2. Fermi National Accelerator Laboratory (FNAL), USA

The FNAL magnetron surface plasma source shown in figure 7, which was developed based on the original 1970s magnetron design from the Soviet Union [41], has provided beams for accelerator operations for over 30 years. When operated with a 15 A discharge current, over 80 mA of H^- beam current is reliably produced at low duty cycles (0.3% @ 15 Hz) with lifetimes exceeding 6 months. This source is currently delivering beams to two accelerator test stands.

FNAL copied the Brookhaven National Laboratory (BNL) developments and made several improvements to the hydrogen and caesium delivery systems to minimise sparking. They have also introduced a solid state high voltage extraction power supply.

3.5.3. Magnetron surface plasma source-BNL, USA

BNL optimised the FNAL design [42]. They reduced the discharge current; increased the extraction voltage and used permanent magnets. This highly reliable, very efficient magnetron is shown in figure 8. This source still regularly provides beam for accelerator operations. A solid state high voltage extraction power supply is also being developed.

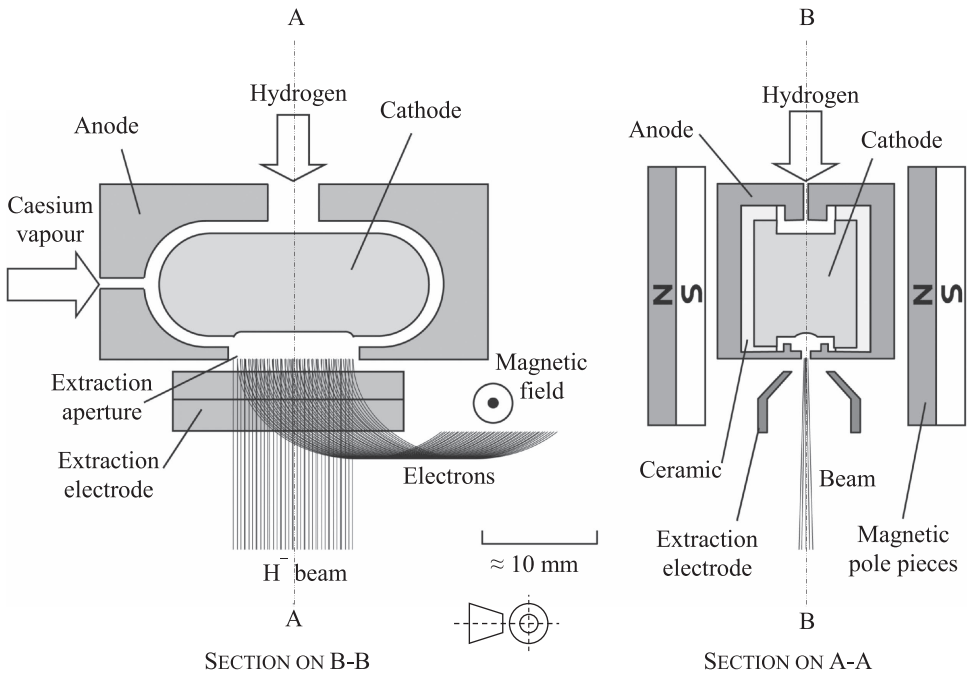

Figure 6. Schematic of a magnetron surface plasma source.

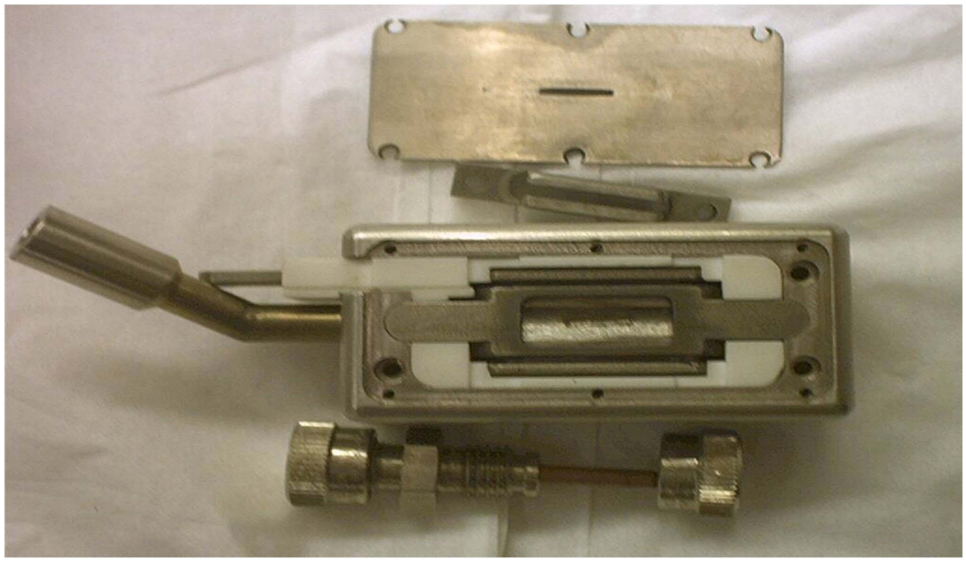

Figure 7. The FNAL surface plasma magnetron source. Reproduced with permission from Fermi National Accelerator Laboratory.

3.6. Penning surface plasma sources

3.6.1. Generalised description

The Penning surface plasma source has a small brick-shaped discharge, bounded by a window-frame anode and two opposing cathodes. Caesium vapour from an external oven and hydrogen and are fed through holes in the anode as shown in figure 9, however it is also possible to feed the discharge through holes in the cathode. A magnetic field is applied perpendicular to the cathode surfaces. The magnetic field confines the electrons to oscillate between the two cathodes. Power is applied to the discharge between the anode and cathode using a current regulated power supply. Beam is extracted through a hole in the anode. An extraction electrode is used to create the electric field that extracts and shapes the beam from the extraction hole.

H^- ions desorbed from the cathode have no direct line of sight to the outlet aperture, so must undergo resonant charge exchange with slow neutral hydrogen atoms to reach the extraction hole. This process yields a beam with low energy spread and emittance, making a high quality beam at high duty factors.

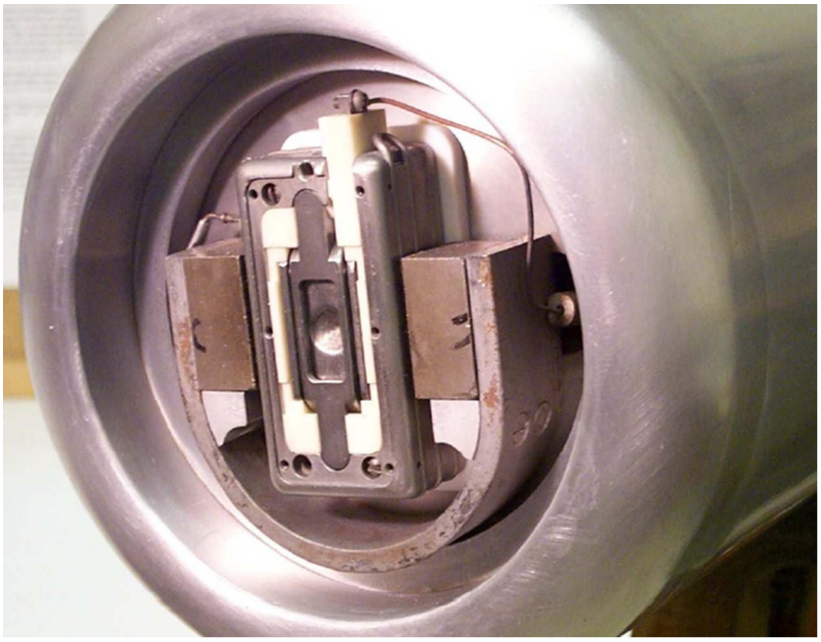

Figure 8. The BNL magnetron surface plasma source with the anode cover plate and extraction electrode removed. Reproduced with permission from Brookhaven National Laboratory.

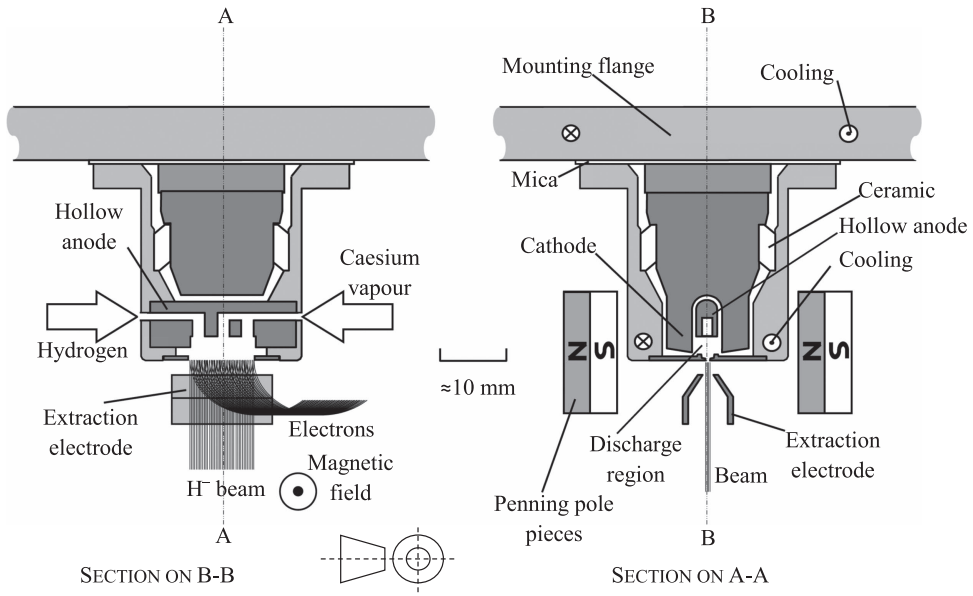

Figure 9. Schematic of a Penning surface plasma source.

3.6.2. ISIS accelerator at the STFC Rutherford Appleton Laboratory (RAL), UK

The ISIS source plasma chamber geometry shown in figure 10, is essentially unchanged from the LANL Penning source of the 1980s [43], itself derived from the original Penning ion source developed by Dudnikov in the 1970s [44]. With 30 years of operational experience, the ISIS design has been replicated in several facilities [45, 46] due to its high emission current density, low emittance, reasonable lifetime, simple operation, rapid replacement and relatively low cost. The ISIS ion source has undergone significant development over the last ten years, primarily to deliver a 60 mA, 10% beam duty cycle, low emittance H^- beam for the Front End Test Stand (FETS) project [47]. The source is currently limited to producing a 60 mA, 5% duty factor beam at 65 keV. To achieve the full 10% duty cycle, a 2X Scaled Penning source is being developed at RAL [48]. Scaling of Penning Surface Plasma Sources was investigated at Los Alamos National Laboratory [49] in the 1990s.

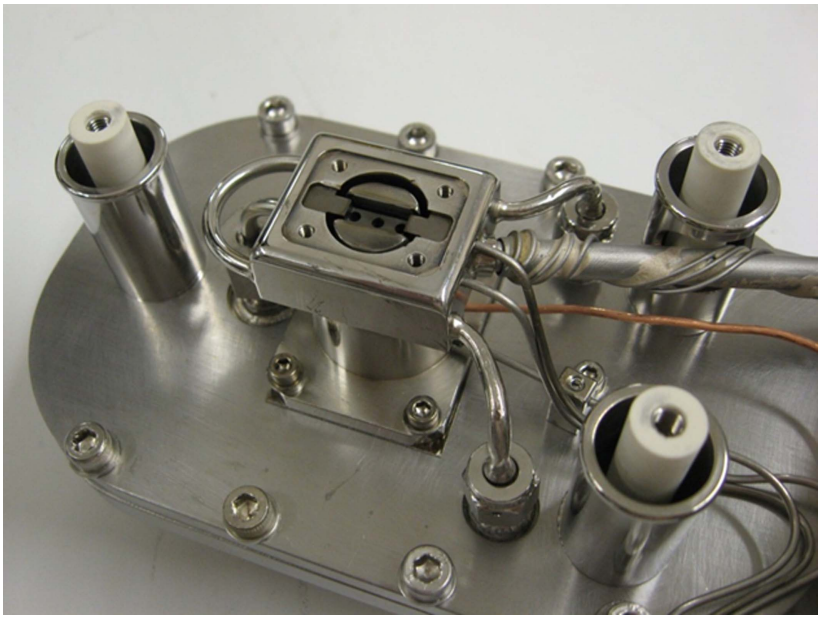

Figure 10. The ISIS Penning H^- ion source with the anode cover plate and extract electrode removed.

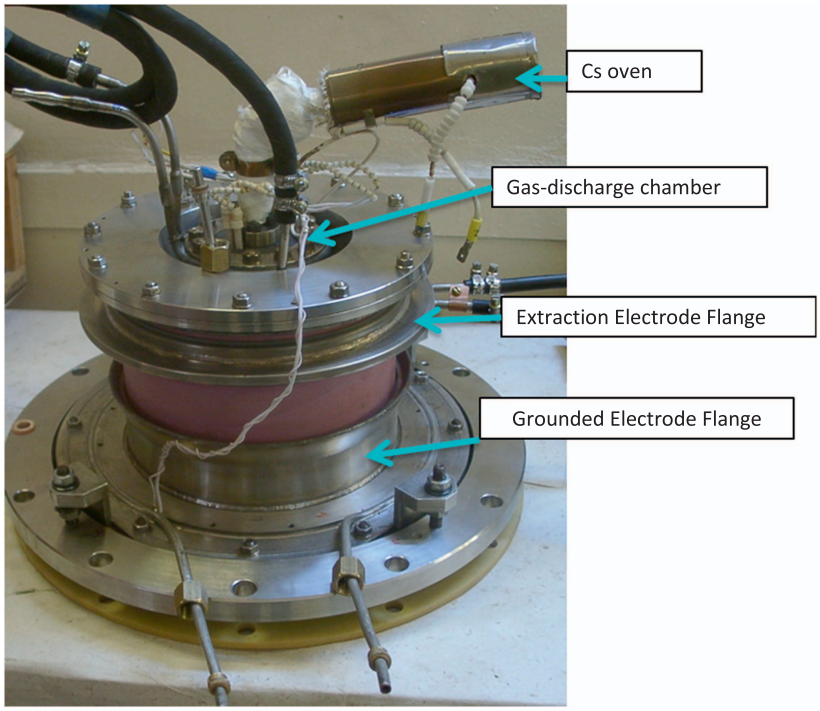

Figure 11. The BINP CW Penning SPS H^- ion source. Reproduced with permission from Budker Institute of Nuclear Physics.

3.6.3. Budker Institute of Nuclear Physics (BINP), Russia

Since 2006 BINP have operated a high current hollow cathode CW Penning source for the Vacuum Insulation Tandem Accelerator. Shown in figure 11, it regularly produces 8 mA CW H^- beam currents at 25 keV [50]. More than 5 mA proton beam current is obtained at the tandem output [51]. A new 15 mA version of the source was developed in 2009. CW currents of 15 mA at 32 keV have been demonstrated in long-term CW runs with source lifetimes >100 h [52]. In 2 h tests, with electrode reinforcement and with the emission aperture increased in diameter to 5 mm, CW currents of 25 mA have been demonstrated [53].

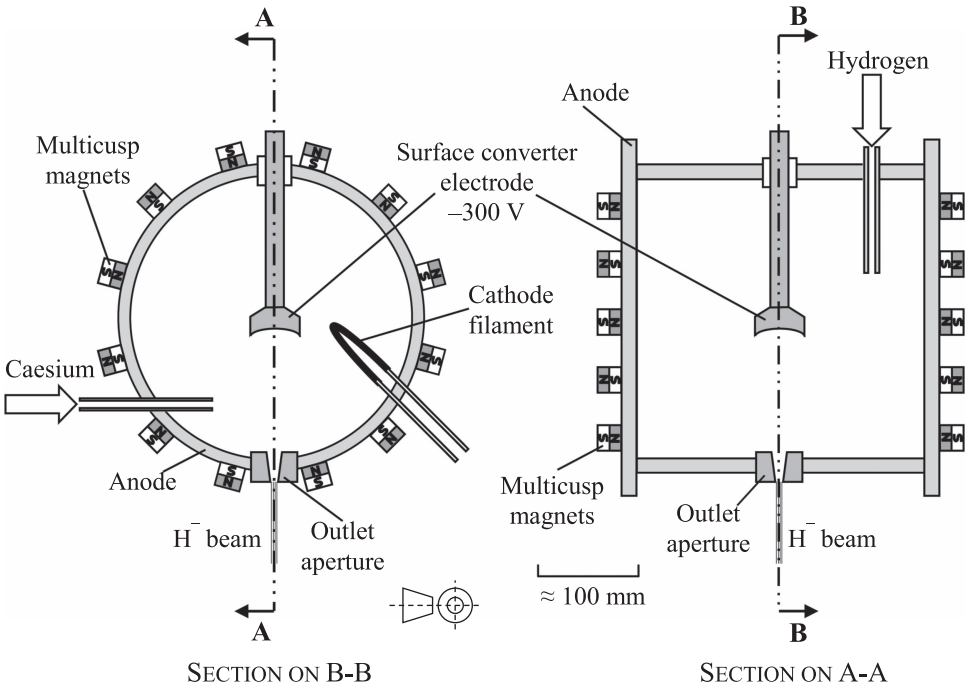

Figure 12. Schematic of a filament driven surface converter source.

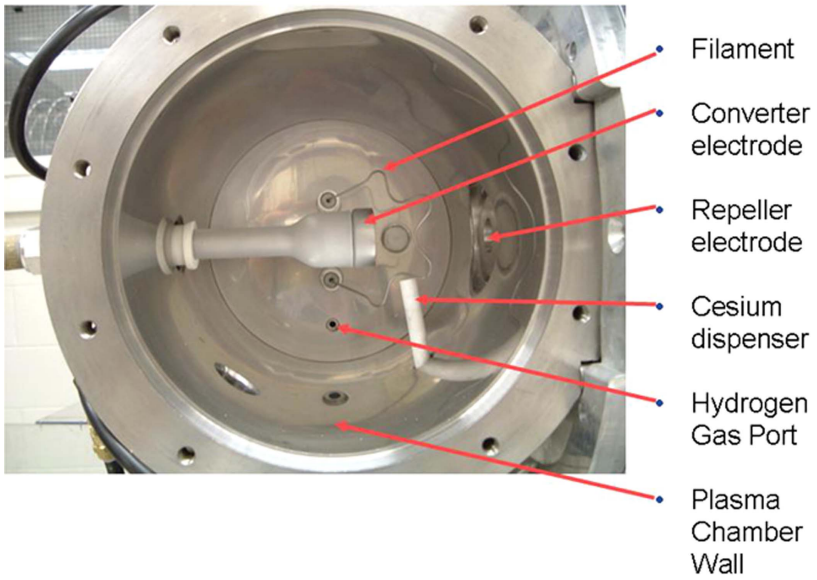

Figure 13. The LANSCE filament driven surface converter source. Reproduced with permission from Los Alamos National Laboratory.

3.7. Filament driven surface converter sources

3.7.1. Generalised description

The filament-driven surface converter source shown in figure 12, has a cylindrical plasma discharge and a concave converter surface on which the H^- ions are produced. The converter surface is located inside the plasma and is biased negatively at a few hundred volts. The converter surface is concave so the H^- ions produced there are focused toward the extraction aperture. Caesium vapour (from an external oven) and hydrogen are fed into the discharge through holes. The plasma chamber wall is the anode and the cathode is a heated filament. The plasma discharge is created by applying power between the anode and cathode. The walls of the vessel are lined with a multicusp magnetic field arrangement to confine the plasma.

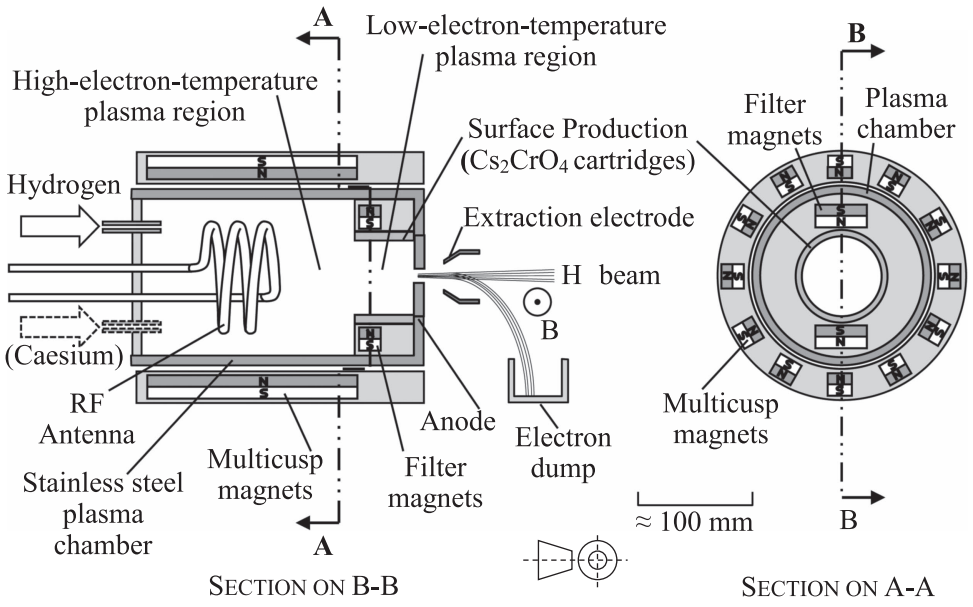

Figure 14. Schematic of an internal RF solenoid antenna driven surface and volume source.

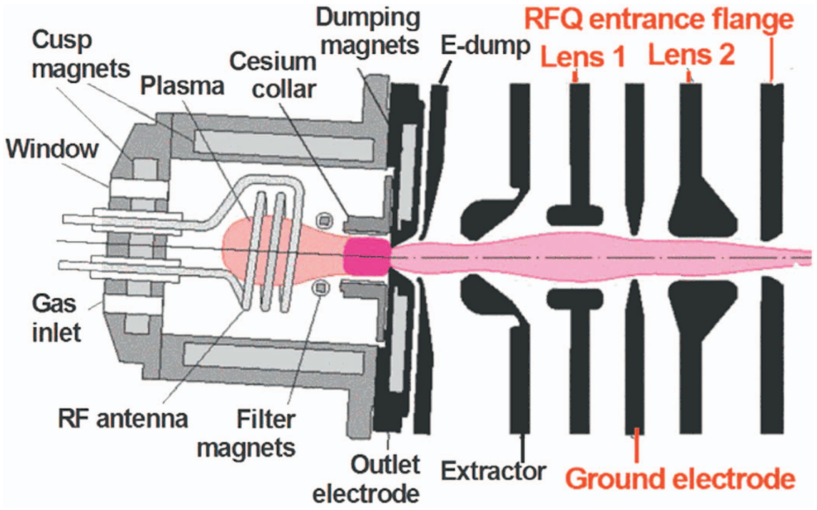

Figure 15. The ORNL SNS internal antenna source. Reproduced with permission from Oak Ridge National Laboratory.

3.7.2. Los Alamos Neutron Science Center (LANSCE), USA

The LANSCE source shown in figure 13, routinely produces a 16 mA, 60 Hz H^- beam with a lifetime of 35 d. Like all filament-driven discharge sources it suffers from lifetime limitations due to filament erosion. A 6 kW pulsed discharge is ignited from a specially shaped tungsten filament. The set-up and stabilisation time of this source takes around 36 h but it can operate at a wide variety of repetition rates [54].

3.8. Internal RF solenoid antenna driven volume and surface sources

3.8.1. Generalised description

The internal RF solenoid antenna driven volume and surface source shown in figure 14, has a cylindrical plasma discharge with a magnetic dipole filter field near the emission aperture. The plasma discharge is coupled to a solenoidal helix RF antenna housed inside in the plasma chamber. The antenna is coated with several thin layers of porcelain, to provide around 0.5 mm of insulation from the plasma. Hydrogen is fed into the discharge through a hole in the back wall. The plasma discharge is created by applying power to the antenna using a power regulated amplifier. After extended high-power, high-duty-factor operation, the ultra-high purity gas can no longer be ignited with just pulsed RF, so a low power, high frequency RF signal is constantly applied in parallel to maintain a dim plasma between high power pulses [55]. The walls of the vessel are lined with a multicusp

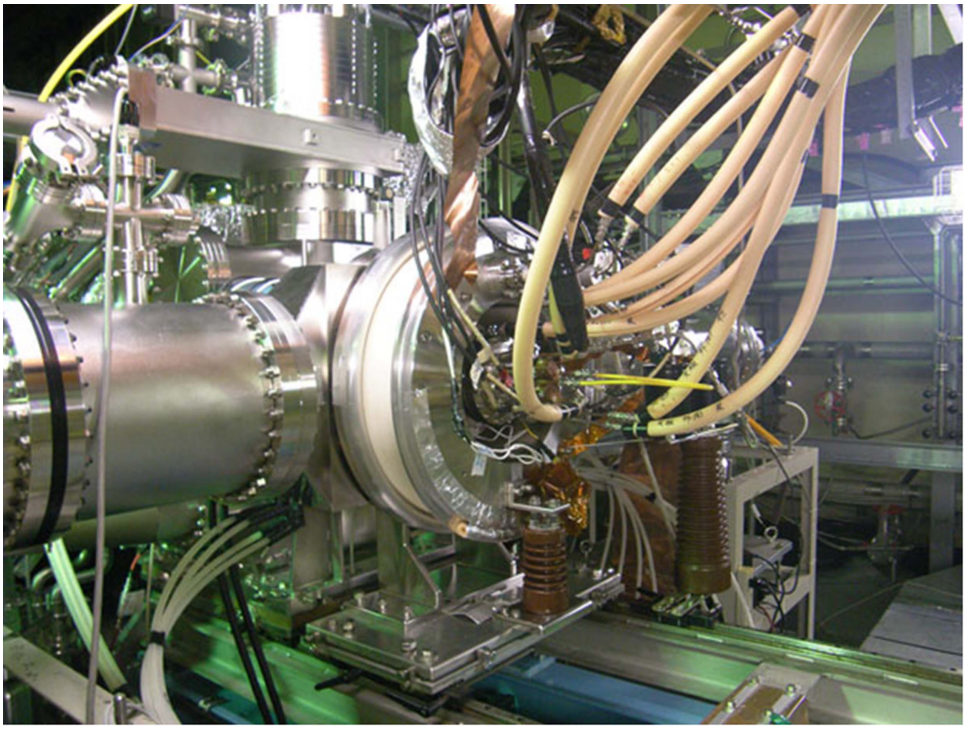

Figure 16. The J-PARC ion source installed on the accelerator. Reproduced with permission from Japan Proton Accelerator Research Complex.

magnetic field arrangement to confine the plasma, whilst separate water-cooled filter magnets are immersed inside the plasma.

This source relies on both volume and surface production processes. Caesium is introduced into the source either by heated caesium chromate (Cs_2CrO_4) cartridges installed in a collar near the emission aperture, or by an external caesium oven. Caesium covers the surfaces near the emission aperture enabling surface production of H^- ions to supplement those produced by the volume process.

3.8.2. Oak Ridge National Laboratory Spallation Neutron Source (ORNL SNS), USA

Shown in figure 15, a 2.5-turn RF antenna is held inside the plasma. The source operates at high duty factors (6%), with a pulsed discharge power of 50–60 kW, and with a temperature-controlled outlet aperture. By using caesium-chromate cartridges housed in the outlet aperture and a precise start-up procedure, this ion source can maintain high beam currents without the need for continual caesium injection. The ion source injects in excess of 60 mA of beam into a compact electrostatic LEBT. The LEBT incorporates two Einzel lenses to match the beam into the following RFQ. The second Einzel lens is split into four quadrants to provide for steering and chopping. The LEBT has no room available for a direct measurement of beam current, for example with a Faraday cup or toroid. Instead, the entrance plane of the RFQ is at floating potential such that beam may be steered onto it using the chopper and steerers as a method of measuring the LEBT output and the RFQ input beam current [56]. Around 35 mA of beam exits the RFQ, whose transmission is sensitive to ion source and LEBT alignment. This is much less than the 56 mA exiting in 2008 [28] before the RFQ transmission started to deteriorate around 2011 [57]. Beam is extracted from the source biased to suit the 65 keV RFQ input energy. To reduce heat loads electrons are dumped immediately outside the source at 6.2 keV, which yields a uniform extraction field and optimises the transmission through the RFQ [28]. Recent performance improvements have focused on reducing electron dump and Einzel lens sparking, strict antenna selection procedures, and ensuring perfect source cleanliness and removal of impurities which would sputter the caesium coverage on the plasma electrode. These improvements have led to long lifetimes of up to 96 d [58], which is world-leading for such a high power, high duty-factor H^- source.

3.8.3. Japan Proton Accelerator Research Complex (J-PARC), Japan

Originally operating with a lanthanum-hexaboride double spiral filament, the J-PARC ion source (figure 16) has been fitted with SNS internal RF antennas. Operating with a thick tapered plasma electrode with a thickness of 16 mm, an external caesium oven, carefully tuned filter magnets and a sophisticated computer-controlled

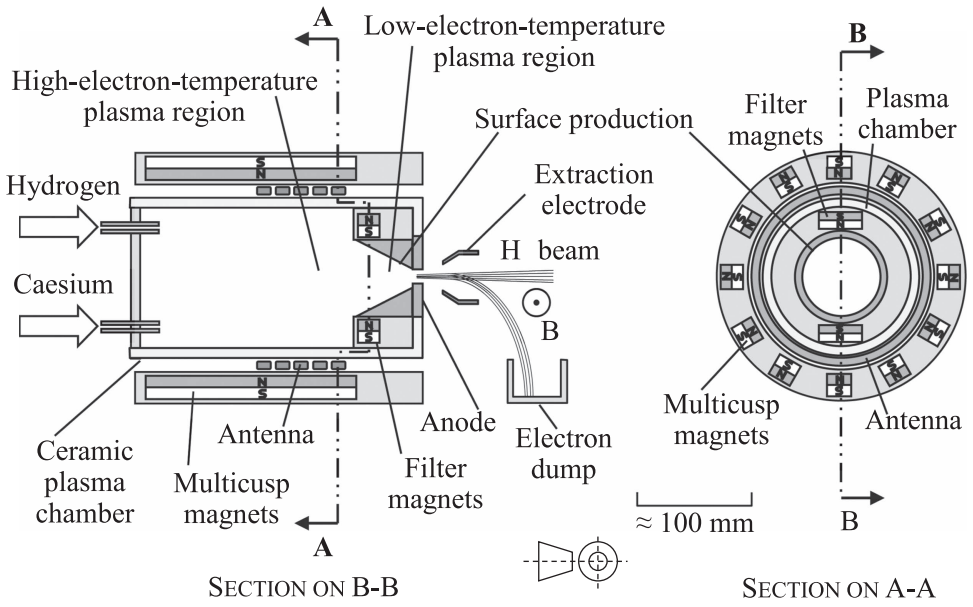

Figure 17. Schematic of an external RF solenoid antenna driven surface and volume source.

feedback system, the J-PARC source is now producing 45 mA of H^- beam current in user operations, with the ability to increase to 66 mA during machine physics periods. The magnetic filter field is produced with two water-cooled rod magnets housed inside the plasma chamber. Beam is produced with a two-stage extraction system, whereby the beam is extracted and co-extracted electrons dumped at 10 keV, then the H^- beam is post-accelerated up to the 50 keV RFQ input energy. Two neighbouring pairs of permanent magnets are housed inside the extraction electrode to produce two consecutive dipole magnetic fields with opposite polarity. The first dipole field dumps the co-extracted electrons and bends slightly the H^- beam. The second dipole field bends back the H^- beam on the beam axis. The ejection angle error of the H^- beam is corrected by an electromagnet, which is located just behind the grounded electrode. A comprehensive improvement campaign involving the emittance reduction by the low plasma electrode temperature operation with slight water feeding into hydrogen plasma, the optimisation of the rod filter magnets, and careful emittance analysis has led to over 66 mA of H^- beam produced in 1000 μs pulses at 25 Hz [59].

3.9. External RF solenoid antenna driven surface and volume sources

3.9.1. Generalised description

The external RF solenoid antenna driven volume source shown in figure 17, also has a cylindrical plasma discharge with a magnetic dipole filter field near the emission aperture, but the plasma discharge is coupled to a solenoidal helix RF antenna outside of the plasma chamber. The antenna is wrapped around the plasma chamber which is made of a dielectric material such as alumina. For higher power operation, aluminium-nitride may be used instead as it has a higher thermal conductivity; however it is more expensive, difficult to machine, and difficult to make a vacuum seal. External antenna RF sources can operate caesium free [14], but for high current/duty cycle operation they rely on both volume and surface production processes. Caesium vapour is fed into the source from an external oven, and covers the surfaces near the emission aperture, enabling surface production of H^- ions. Because the RF must be coupled (with associated losses) into the plasma through ceramic walls, a higher RF power may be required than for internal RF antennas. Another issue is the high inductance of the large solenoid, which can lead to high voltage discharges for high power operations. A separate low power plasma ignition power supply may be required for increased stability.

3.9.2. CERN Linac4, Switzerland

An upgraded copy of the highly successful DESY external antenna source [14], the CERN Linac4 source (figure 18) is designed to operate at a higher duty cycle whilst producing more beam [60]. It uses an octopole cusp field and a five-turn external RF antenna to feed 40 kW of 2 MHz RF power into the plasma. Originally intended to be operated without caesium, as at DESY, the required operational parameters could only be met with the introduction of caesium. A two-day stabilisation period is required after installing the ion source, however persistent beam currents have been demonstrated for seven weeks. Unlike the SNS and J-PARC sources which use a continuous low power RF signal to maintain plasma between high power pulses, the CERN source

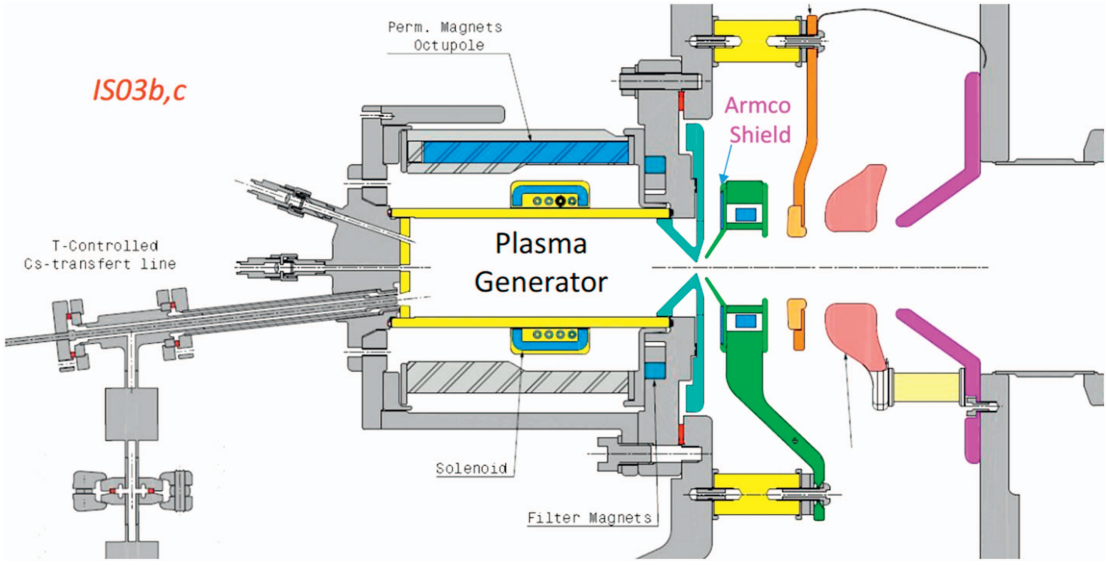

Figure 18. Schematic of CERN's LINAC4 source. Reproduced with permission from CERN.

does not need continual low power injection. Instead, because of its low repetition rate of 0.8 Hz, it is possible to provide a sufficiently high pressure hydrogen gas pulse to initiate plasma breakdown each pulse. Since the pulsed hydrogen pressure varies during the plasma pulse, a sophisticated feedback loop is implemented to adjust the RF power during the pulse such that the resultant beam current has a flat top. The downstream LEBT residual gas pressure is also closely monitored as it affects the beam space-charge neutralisation process, which in turn affects beam transmission through the RFQ. Several iterations of post-extraction optics involving an electron dump and einzel lens have been implemented to enhance the beam transport. Recent research has focused on understanding the plasma pulse through impressive modelling and spectroscopy measurements, as well as investigating the cause of a higher-than-expected beam emittance. The aim is to push the beam current towards 80 mA from its 45 mA present value, whilst maintaining a low emittance.

3.10. Comparative table

Table 1 summarises the performance of the sources detailed in this paper.

4. Discussion

Accelerator facilities require the ion source to be very reliable. The ion source should not be the main cause of failure for the accelerator facility as a whole, otherwise questions will be asked. This has caused a large amount of ion source development activity to be focused on long lifetime sources. Source availability is simply the percentage of time that a source delivers beam when it is scheduled to do so. By scheduling suitably timed maintenance days in an accelerator operations schedule, even sources with relatively short lifetimes can deliver 100% availability. For example, ISIS user cycles are between 4 and 8 weeks in length with a scheduled maintenance day approximately every 2 to 3 weeks. By changing the source during the maintenance day; when the source is only at half its maximum lifetime (~6 weeks); source availabilities of 100% for a user cycle are often achieved. Although the maintenance days were primarily introduced to change the source, they have also proved useful for overall machine operations because they provide opportunity for other equipment to be repaired or inspected. The downsides of this approach are: more sources need to be refurbished; no long term source lifetime statistics can be generated because the sources are never allowed to run to failure; and this approach is only feasible where regular access is available.

The requirements of the accelerator facility dictate which source should be used. For DC beams up to 8 mA the obvious choice is an external planar RF antenna volume source because of its 'maintenance free' operation. However the RF amplifier adds significantly to the cost of the source so where the accelerator schedule allows it, a filament driven volume source is a more cost effective solution for DC beams up to 15 mA. Filaments can be quickly, easily and cheaply replaced. With high discharge powers the volume process can produce at most 40 mA of beam suitable for accelerator applications.

The only way to exceed 40 mA of beam current is to add caesium. This instantly adds handling, management and cleaning complications, resulting in higher costs and complexity. With the addition of caesium and a

Table 1. Comparison of sources currently operating on accelerator facilities or accelerator test stands.

Source	Variant	Technology	Caesium	Discharge	Beam duty cycle	Beam current	Extraction aperture	Lifetime	4·RMS normalised emittance
D-Pace	Filament	Filament-driven volume	No	47.5 A 120 V	100%	18 mA	11.3 mm diameter	> 5250 mA h	0.8 π mm mrad
D-Pace	RF	External planar antenna RF-driven volume	No	3 kW 13.56 MHz RF	100%	8 mA	7.0 mm diameter	> 1 year	0.6 π mm mrad
ISIS	Operations	Penning surface plasma	Yes, elemental	55 A 70 V	1.5% @ 50 Hz	55 mA	(0.6 mm × 10 mm) Slit	5 weeks	1.0 π mm mrad
ISIS	FETS	Penning surface plasma	Yes, elemental	55 A 70 V	10% @ 50 Hz	80 mA	(0.6 mm × 10 mm) Slit	2 weeks	1.2 π mm mrad
BINP	CW	Penning surface plasma	Yes, caesium chromate	11 A 70 V	100% CW	25 mA	5.0 mm diameter	>100 h @15 mA	1.2 π mm mrad
FNAL	Operations	Magnetron surface plasma	Yes, elemental	15 A 180 V	0.3% @ 15 Hz	80 mA	3.2 mm diameter	9 months	0.8 π mm mrad
BNL	Operations	Magnetron surface plasma	Yes, elemental	18 A 140 V	0.5% @ 7.5 Hz	100 mA	2.8 mm diameter	6 months	1.6 π mm mrad
LANL	LANSCE	Filament-driven surface convertor	Yes, elemental	45 A 200 V	5% @ 60 Hz	18 mA	9.8 mm diameter	5 weeks	0.8 π mm mrad
SNS	Operations	Internal solenoid antenna RF-driven volume and surface	Yes, caesium chromate	Pulsed 60 kW 2 MHz RF + CW 300 W 13 MHz RF	6% @ 60 Hz	>60 mA	7.0 mm diameter	14 weeks	~1 π mm mrad
J-PARC	Operations	Internal solenoid antenna RF-driven volume and surface	Yes, elemental	Pulsed 36 kW 2 MHz RF + CW 50 W 30 MHz RF	1.25% @ 25 Hz (test stand 2.5% @ 25 Hz)	45 mA (test stand 66 mA)	9.0 mm diameter	8 weeks	0.9 π mm mrad
CERN	Linac4	External solenoid antenna RF-driven volume and surface	Yes, elemental	Pulsed 40 kW 2 MHz RF	0.03% @ 0.8 Hz	45 mA	5.5 mm diameter	7 weeks	1.2 π mm mrad

suitable surface production region near the extraction aperture, beam currents of 80 mA can be extracted from combined volume and surface sources. This makes the RF volume and surface sources the best choice for 40–80 mA operation.

The highest brightness beams are produced by the Penning and magnetron surface plasma sources. With current densities measured in the A cm^{-2} range, they are the only sources that can produce beam currents in excess of 100 mA. However surface plasma sources are fundamentally lifetime limited by the sputtering rate of molybdenum electrodes, yielding short lifetimes when operated at high currents and duty factors.

Acknowledgements

The authors would like to Yuri Belchenko, Dan Bollinger, Morgan Dehnel, Hidetomo Oguri and Martin Stockli and the referee for their comments and suggestions to help improve this paper.

References

[1] Kurutz U and Fantz U 2015 Investigations on caesium-free alternatives for H^- formation at ion source relevant parameters *AIP Conf. Proc.* **1655** 020005
[2] Vogel J S 2015 H^- formation by neutral resonant ionisation of H($n = 2$) atoms *AIP Conf. Proc.* **1655** 020015
[3] Tarvainen O, Kalvas T, Komppula J, Koivisto H, Geros E, Stelzer J, Rouleau G, Johnson K F and Carmichael J 2011 Effect of ion escape velocity and conversion surface material on H^- production *AIP Conf. Proc.* **1390** 113
[4] Moehs D P, Peters J and Sherman J 2005 Negative hydrogen ion sources for accelerators *IEEE Trans. Plasma Sci.* **33** 1786–98
[5] Peters J 2000 Negative ion sources for high energy accelerators (invited) *Rev. Sci. Instrum.* **71** 1069–74
[6] Maazouz M, Borisov A G, Esaulov V A, Gauyacq J P, Guillemot L, Lacombe S and Teillet-Billy D 1997 Effect of metal band characteristics on resonant electron capture: H^- formation in the scattering of hydrogen ions on Mg, Al and Ag surfaces *Phys. Rev.* B **55** 13869–77
[7] Borisov A G, Teillet-Billy D and Gauyacq J P 1992 H^- formation by electron capture in hydrogen–Al(111) collisions: perturbative and nonperturbative approaches *Surf. Sci.* **278** 99–110
[8] Dudnikov V 2012 Forty years of surface plasma source development *Rev. Sci. Instrum.* **83** 02A708
[9] Bacal M and Wada M 2015 Negative hydrogen ion production mechanisms *Appl. Phys. Rev.* **2** 021305
[10] Lawrie S R, Faircloth D C, Letchford A P, Perkins M, Whitehead M O, Wood T, Gabor C and Back J 2014 Development of the front end test stand and vessel for extraction and source plasma analyses negative hydrogen ion sources at the Rutherford Appleton Laboratory *Rev. Sci. Instrum.* **85** 02B127
[11] Bollinger D S, Karns P R and Tan C Y 2015 Reduction of beam current noise in the FNAL magnetron *AIP Conf. Proc.* **1655** 070002
[12] Draganic I N, O'Hara J F O and Rybarcyk L J 2016 Different approaches to modeling the LANSCE H^- ion source filament performance *Rev. Sci. Instrum.* **87** 02B112
[13] Kuo T, Yuan D, Jayamanna K, McDonald M, Baartman R, Schmor P and Dutto G 1996 On the development of a 15 mA direct current H^- multicusp source *Rev. Sci. Instrum.* **67** 1314–6
[14] Peters J 2009 The new DESY RF-driven multicusp H^- ion source *AIP Conf. Proc.* **1097** 171
[15] Fantz U, Heinemann B, Wunderlich D, Riedl R, Kraus W, Nocentini R and Bonomo F 2016 Towards 20 A negative hydrogen ion beams for up to 1 h: achievements of the ELISE test facility (invited) *Rev. Sci. Instrum.* **87** 02B307
[16] Stockli M P, Han B, Murray S N, Pennisi T R, Piller C, Santana M and Welton R 2016 Recent performance of and plasma outage studies with the SNS H^- source *Rev. Sci. Instrum.* **87** 02B140
[17] Lettry J 2016 Linac4 H^- ion sources *Rev. Sci. Instrum.* **87** 02B139
[18] Chou S H and Voss J 2012 An orbital-overlap model for minimal work functions of cesiated metal surfaces *J. Phys.: Condens. Matter* **24** 445007
[19] Faircloth D C, Lawrie S R, Pereira Da Costa H and Dudnikov V 2015 Operational and theoratical temperature considerations in a Penning surface plasma source *AIP Conf. Proc.* **1655** 030013
[20] Ueno A, Namekawa Y, Yamazaki S, Ohkoshi K, Koizumi I, Ikegami K, Takagi A and Oguri H 2013 Over 60 mA RF-driven H^- ion source for the J-PARC *AIP Conf. Proc.* **1515** 331
[21] Lettry J 2014 Status and operation of he Linac4 ion source prototypes *Rev. Sci. Instrum.* **85** 02B122
[22] Sosa A, Bollinger D S, Duel K, Karns P R, Pellico W and Tan C Y 2016 An overview of the new test stand for H^- ion sources at FNAL *Rev. Sci. Instrum.* **87** 02B105
[23] Belchenko Y, Gorbovsky A, Sanin A and Savkin V 2014 The 25 mA continuous-wave surface-plasma source of H^- ions *Rev. Sci. Instrum.* **85** 02B108
[24] Stockli M P, Han B X, Murray S N, Pennisi T R, Santana M and Welton R F 2013 Recent performance of the SNS H^- source for 1 MW neutron production *AIP Conf. Proc.* **1515** 292
[25] Fantz U, Friedl R and Froschle M 2012 Controllable evaporation of cesium from a dispenser oven *Rev. Sci. Instrum.* **83** 123305
[26] Friedl R and Fantz U 2015 Temperature dependence of the work function of caesiated materials under ion source conditions *AIP Conf. Proc.* **1655** 020004
[27] Belchenko Y I, Gorbovsky A I, Ivanov A A, Konstantinov S G, Sanin A L, Shikhovtsev I V and Tiunov M A 2013 Multiaperture negative ion source *AIP Conf. Proc.* **1515** 167
[28] Stockli M P, Han B, Murray S N, Pennisi T R, Santana M and Welton R F 2010 Ramping up the spallation neutron source beam power with the H^- source using 0 mg Cs/Day *Rev. Sci. Instrum.* **81** 02A729
[29] Kapchinskij I and Vladimirskij V 1959 *Proc. of the Int. Conf. on High Energy Accelerators and Instrumentation* (Geneva: CERN)
[30] Reiser M 2008 *Theory and Design of Charged Particle Beams* 2 edn (Weinheim: Wiley)
[31] Lapostolle P M 1971 Possible emittance increase through filamentation due to space charge in continuous beams *IEEE Trans. Nucl. Sci.* **18** 1101–4
[32] Stockli M P, Welton R F, Keller R, Letchford A P, Thomae R W and Thomason J W G 2002 Accurate estimation of the RMS emittance from single current amplifier data *AIP Conf. Proc.* **639** 135

[33] D-Pace 2017 15 mA H^- ion source, Turnkey system, [Online] (http://d-pace.com/images/products/Ion%20Sources/F.H-15.30-SYS/spec/2120038_r1.2-ion-source-turnkey-15-ma-h-.pdf) (Accessed: April 2017)
[34] Etoh H *et al* 2017 Development of a 20 mA negative hydrogen ion source for cyclotrons *AIP Conf. Proc.* **1869** 030050
[35] Kalvas T, Tarvainen O, Komppula J, Koivisto H, Tuunanen J, Potkins D, Stewart T and Dehnel M P 2015 A CW radiofrequency ion source for production *AIP Conf. Proc.* **1655** 030015
[36] D-Pace 2017 7.5 mA H^- RF ion source, Turnkey, [Online] (http://d-pace.com/images/products/Ion%20Sources/RF.H-7.5-30-SYS/spec/2120046_r0.3-rf-ion-source-turnkey-7.5-ma-h-.pdf) (Accessed: April 2017)
[37] Melanson S, Dehnel M, Potkins D, McDonald H and Philpott C 2017 H^-, D^-, C_2^-: a comparison of RF and filament powered volume-cusp ion sources *IPAC (Copenhagen)*
[38] Tarvainen O and Peng S X 2016 Radiofrequency and 2.45 GHz electron cyclotron resonance H^- volume production ion sources *New J. Phys.* **18** 105008
[39] Spence D and Lykke K R 1998 *Proc. 19th Linear Accelerator Conf. (LINAC) (Chicago, IL, USA)* TU4048 (www.jacow.org)
[40] Gobin R, Auvray P, Bacal M, Breton J, Delferriere O, Harrault F, Ivanov A, Svarnas P and Tuske O 2006 Two approaches for H^- ion production with 2.45 GHz ion sources *Nucl. Fusion* **46** S281–6
[41] Belchenko Y I, Dimov G I and Dudnikov V G 1974 A powerful injector of neutrals with a surface-plasma source of negative ions *Nucl. Fusion* **14** 113
[42] Alessi J G 2002 *High AND High Brightness Hadron Beams: 20th ICFA Advanced Beam Dynamics Workshop on High Intensity and High Brightness Hadron Beams ICFA-HB2002*
[43] Allison P W 1977 A direct extraction H^- ion source *IEEE Trans. Nucl. Sci.* **24** 1594–6
[44] Dudnikov V 1974 Surface-plasma source of negative ions with a Penning discharge *Proc. of the 4th All-Union Conf. on Charged Particle Accelerators (Moscow)*
[45] Bustinduy I *et al* 2010 First simulation tests for the Bilbao accelerator ion source test stand *Proc. of the Int. Particle Accelerator Conf. (Kyoto, Japan)*
[46] Ouyang H *et al* 2010 The development of the H^- ion source test stand for CSNS *Proc. of LINAC10* September 2010
[47] Faircloth D C, Lawrie S R, Letchford A P, Gabor C, Whitehead M, Wood T and Perkins M 2011 Latest results from the front end test stand high performance H^- ion source at RAL *AIP Conf. Proc.* **1390** 205
[48] Rutter T, Faircloth D, Turner D and Lawrie S 2015 The mechanical design and simulation of a scaled H^- Penning ion source *Rev. Sci. Instrum.* **87** 02B131
[49] Vernon Smith H Jr *et al* 1992 Penning surface-plasma source scaling laws—theory and practice *AIP Conf. Proc.* **287** 271
[50] Belchenko Y, Sanin A, Gusev I, Khilchenko A, Kvashnin A, Rashchenko V, Savkin V and Zubarev P 2008 Direct current H^- source for boron neutron capture therapy tandem accelerator *Rev. Sci. Instrum.* **79** 02A521
[51] Ivanov A A, Kasatov D A, Koshkarev A M, Makarov A N, Ostreinov Y M, Sorokin I N, Taskaev S Y and Shchudlo I M 2016 Obtaining a proton beam with 5 mA current in a tandem accelerator with vacuum insulation *Tech. Phys. Lett.* **42** 608–11
[52] Belchenko Y, Sanin A and Ivanov A 2008 A 15 mA CW H^- source for accelerators *AIP Conf. Proc.* **1097** 214
[53] Belchenko Y, Gorbovsky A, Sanin A and Savkin V 2014 The 25 mA continuous-wave surface-plasma source of H ions *Rev. Sci. Instrum.* **85** 02B108
[54] Keller R, Tarvainen O, Chacon-Golcher E, Geros E G, Johnson K F, Rouleau G, Stelzer J E and Zaugg T J 2009 H^- ion source development for the LANSCE accelerator systems *AIP Conf. Proc.* **1097** 161
[55] Stockli M P, Han B X, Murray S N, Pennisi T R, Piller C, Santana M and Welton R 2015 Recent performance and ignition tests of the pulsed SNS H^- Source for 1 MW neutron production *AIP Conf. Proc.* **1655** 030001
[56] Han B X, Welton R F, Murray S N Jr, Pennisi T R, Santana M, Stinson C M and Stockli M P 2017 Refined beam measurements on the SNS injector *AIP Conf. Proc.* **1869** 030014
[57] Stockli M P, Ewald E D, Han B X, Murray S N Jr, Pennisi T R, Piller C, Santana M, Tang J and Welton R Recent performance of the SNS H^- ion source and low-energy beam transport system *Rev. Sci. Instrum.* **85** 02B137
[58] Stockli M P, Han B X, Welton R F, Murray S N Jr, Pennisi T R, Santana M, Stinson C M and Stockli M P 2017 Record performance of and extraction studies with the Spallation Neutron Source H^- injector *AIP Conf. Proc.* **1869** 030010
[59] Ueno A 2017 Cesiated surface H^- ion source: optimization studies *New J. Phys.* **19** 015004
[60] Lettry J *et al* 2017 CERN's Linac4 cesiated surface H^- source *AIP Conf. Proc.* **1869** 030002